

# Effects of Measurement Materials and Oxygen Partial Pressure on Synthetic Coal Slag Viscosity Values

Jingxi ZHU<sup>\*1,2</sup>, Tetsuya Kenneth KANEKO<sup>1,2</sup>, Haoyuan MU<sup>2</sup>, James P. BENNETT<sup>3</sup> and Seetharaman SRIDHAR<sup>1,2</sup>

1) US Department of Energy, National Energy Technology Laboratory, Pittsburgh, PA 15236, USA

2) Department of Materials Science and Engineering, Carnegie Mellon University, Pittsburgh, PA 15213, USA

3) US Department of Energy, National Energy Technology Laboratory, Albany, OR 97321 USA

**Abstract:** The viscosity of the molten ash (slag) resulting from the mineral constituents in slagging gasifiers is critical for controlling the operation of the process. The viscosity of two synthetic slags with compositions resembling the mineral impurity constitution of coal feedstocks were examined at temperatures from 1300~1500 °C using a rotating-bob viscometer. A few combinations of atmospheres and experimental materials were investigated with respect to one another to determine slag viscosity. A CO/CO<sub>2</sub> atmosphere (CO:CO<sub>2</sub>=1.8, corresponding to P<sub>O2</sub>=10<sup>-8</sup> atm) is required to sustain ferrous ions in FeO-containing slags, however it is oxidizing to most metals. Iron oxide in the slag prevents usage of Fe parts. In un-purified Ar, the Fe metal surface oxidizes. Utilizing purified argon prevents iron measurement components from oxidation, however, the metallic surfaces act as nucleation sites for the reduction of the Fe-oxide in the slag into metallic Fe. Dissolution of ceramic materials, including Al<sub>2</sub>O<sub>3</sub> and ZrO<sub>2</sub>, occurs in both atmospheres. Therefore, evaluating slag properties in the laboratory is challenging. The measured viscosities diverged depending on the material selection. This difference is likely attributable to the container/spindle-slag interaction. The measurements with ceramic parts agreed best with FactSage prediction, with an average activation energy of 271.2 kJ for eastern coal slag. The dissolution of container/spindles materials was substantial during measurement of western coal slag, and precipitation of crystalline phase was inevitable. Nevertheless, the viscosity data agreed best with Kalmanovitch prediction above 1350°C. The activation energy changed dramatically for both datasets, likely indicating the Newtonian-to-non-Newtonian transition.

**Keywords:** coal gasifier, viscosity, measurement components, crystallization

## 1. Introduction

Gasification allows for the generation of power from lower cost solid fuels such as western coal and petcoke. Among various technologies, high-temperature slagging gasifiers have the potential to co-gasify fuels such as petroleum byproducts and biomass waste; which would increase fuel flexibility, lower the net CO<sub>2</sub> output and emissions, and be adaptable to carbon capture and storage (CCS) to achieve near-zero air emissions. In integrated gasification combined cycle (IGCC) power systems, the pollutants are converted into re-usable byproducts and the excess heat is used in a steam turbine. However, issues related to maintenance and reliability of the gasifier need to be addressed. The difficulties are largely related to the inorganic constituents in the fuel feedstock. In a slagging/entrained flow gasification system, the inorganic constituents leave the gasifier as a molten slag. Carbon feedstock materials; which can include coal, petroleum coke (petcoke), biomass, or mixtures of these materials; contain numerous minerals that liquefy under the gasification conditions [T = 1325 to 1600 °C, P = 2.07 – 6.89 MPa, and log(P<sub>O2</sub>) = -9 to -7].<sup>[1]</sup> The

liquefied ash coalesces and forms a slag. The composition, structure and resulting properties of the slag are critical to the operation of the gasifier. Depending on the slag properties; it can either be too viscous and clog slag flow from the gasifier, or be too fluid and cause excessive degradation of the refractory liner.<sup>[2]</sup> Improvements in both of these areas can enhance the commercial competitiveness of IGCC technology, which in turn can lead to improved economics of its use with Carbon Capture and Sequestration (CCS).

Slag viscosity and precipitation kinetics are impacted by the degree of polymerization and the size and shape of the polymeric units. Both of these structural features will vary as the slag drains downwards along the sidewall or infiltrates into the refractory. They will also vary according to the partial pressure of oxygen, which is determined by the CO/CO<sub>2</sub> ratio in the gasifier. Ash composition depends on the source of the coal and/or any additional carbonaceous feedstock such as petcoke. For example westerns US coal, compared to eastern US coal, is significantly richer in CaO, which is a strong de-polymerizing unit.<sup>[3]</sup> Eastern coal, on the other hand, contains significant amounts of Fe-oxides, but their de-polymerizing ability depends on the oxidation state of Fe, and is influenced by the oxygen partial pressure. Evaluations of molten coal-ash viscosity were abundant for binary (such as CaO-SiO<sub>2</sub>, FeO-SiO<sub>2</sub> and Al<sub>2</sub>O<sub>3</sub>-SiO<sub>2</sub>), ternary (such as CaO-FeO-SiO<sub>2</sub>, FeO-SiO<sub>2</sub> and Al<sub>2</sub>O<sub>3</sub>-CaO-SiO<sub>2</sub>), quaternary (such as Al<sub>2</sub>O<sub>3</sub>-CaO-FeO-SiO<sub>2</sub>) and high-order systems.<sup>[4]</sup> A lot of these studies have been conducted under inert atmospheres using rotating bob viscometry using either metallic (Mo or Fe) or ceramic materials in contact with the slag. Several estimation models have been proposed such as Urbain<sup>[5]</sup>, Browning<sup>[2]</sup>, FactSage<sup>[6]</sup> and Kalmanovitch<sup>[7]</sup> models.

The aim of this work is to measure viscosities of synthetic slags with compositions corresponding to ash from two US coal sources (western and eastern) under thermal and atmospheric conditions that are similar to those in a gasifier. Most significantly, this constraint entails carrying out the measurements under a CO/CO<sub>2</sub> ratio of 1.8, which corresponds to an oxygen partial pressure of 10<sup>-8</sup> atm. This selection in atmosphere poses a challenge with respect to the optimal selection of materials for the crucibles and spindles that are in contact with the melt. The atmosphere is oxidizing with respect to iron and molybdenum, while ceramic parts can dissolve into the slag. Therefore, purified Ar atmosphere must be used for metallic parts. Platinum is problematic at high Fe-oxide content, which has Fe dissolution into the Pt.<sup>[8]</sup> Specifically we aim to address the following:

- (i) Establish whether measurements carried out in inert atmospheres cause FeO conversion into Fe within the time of the measurement and whether this influences the measured viscosity.
- (ii) Whether excessive dissolution of ceramic parts (Al<sub>2</sub>O<sub>3</sub> and ZrO<sub>2</sub>) into the slag alters the slag chemistry and measured viscosity.
- (iii) Whether the measured viscosities of synthetic slags with chemistries similar to US coal ashes agree with the available model predictions.

## **2. Experimental**

### **2.1 Sample preparation**

Two synthetic slags with compositions resembling the mineral impurity constitution of United States coal feedstocks

in entrained-flow slagging gasifiers were used in this investigation. First, a representative slag composition was selected by taking an average of ash constituents derived from sub-bituminous coal feedstock from the United States, which will be referred to as eastern coal (EC) from hereon. This slag was used for the majority of the experiments. Secondly, a slag representing the ash composition of coal from western United States (WC) was designed.<sup>[3]</sup> The individual oxide components in powder form were mixed to their appropriate ratios and melted and equilibrated in a gas mixture of CO/CO<sub>2</sub> with a ratio of 1.8, corresponding to an oxygen partial pressure of 10<sup>-8</sup> atm. FactSage calculations indicated that at the particular oxygen partial pressure, the Fe-oxide should be 99.92 at% in the form of FeO and 0.08 at% in the form of Fe<sub>2</sub>O<sub>3</sub>. Upon extracting the vitreous material from the crucible, it was ground to particles roughly 2 mm in size. For the Eastern coal slag, dissolution of the Al<sub>2</sub>O<sub>3</sub> crucible was minimal with roughly a 1 wt% increase in Al<sub>2</sub>O<sub>3</sub> concentration observed. On the contrary, Al<sub>2</sub>O<sub>3</sub> crucible dissolution was more substantial with the western coal, with approximately a 5 wt% increase in Al<sub>2</sub>O<sub>3</sub> concentration noted in the slag.

The starting slag compositions are listed in Table 1, as well as the compositions of the spent slags, which were measured in post-viscosity experiments. The slag compositions were evaluated using X-ray fluorescence (XRF) spectrometry. The letter “B” in the sample labels stands for “batch” and is followed by the batch number. The virgin slag of each batch is labeled “BX-VS”; with “M” standing for post measurement slag, followed by the measurement number. Eastern coal slags are labeled with “EC” and western coal slags with “WC”.

Table 1 Chemical analysis of starting and spent slags for both a) eastern coal slag and b) western coal slag

a)								b)			
wt%	EC-B1-VS	EC-B1-M1	EC-B1-M3	EC-B2-VS	EC-B2-M1	EC-B2-M2	EC-B2-M3	wt%	WC-B1-VS	WC-B1-M1	WC-B1-M2
Al <sub>2</sub> O <sub>3</sub>	27.33	27.38	27.54	26.02	26.72	26.07	26.29	Al <sub>2</sub> O <sub>3</sub>	21.69	31.12	23.21
CaO	6.15	6.06	6.11	6.54	6.5	6.52	6.44	CaO	25.77	22.5	20.9
Fe <sub>2</sub> O <sub>3</sub>	17.05	16.61	16.17	18.42	18.31	18.28	18.18	Fe <sub>2</sub> O <sub>3</sub>	10.53	9.3	8.41
K <sub>2</sub> O	2.52	2.24	2.32	2.24	2.23	2.23	2.23	K <sub>2</sub> O	1.41	1.19	1.13
MgO	1.21	1.2	1.2	1.28	1.26	1.29	1.26	MgO	6.05	5.42	5.28
MnO	0.043	0.045	0.19	0.042	0.042	0.044	0.042	MnO	0.098	0.086	0.086
Na <sub>2</sub> O	0.72	0.79	0.82	0.75	0.75	0.82	0.79	Na <sub>2</sub> O	5.25	4.58	4.2
P <sub>2</sub> O <sub>5</sub>	0.008	0.031	0.02	0.022	0.023	0.027	0.024	P <sub>2</sub> O <sub>5</sub>	0.017	0.016	0.039
SiO <sub>2</sub>	44.85	45.14	45.35	44.47	44	44.35	44.55	SiO <sub>2</sub>	28.87	25.49	26.83
TiO <sub>2</sub>	0.08	0.06	0.066	0.085	0.067	0.067	0.069	TiO <sub>2</sub>	0.033	0.036	0.037
ZrO <sub>2</sub>	0.038	0.37	0.13	0.035	0.026	0.23	0.029	ZrO <sub>2</sub>	0.07	0.004	9.64

Fig. 1 shows the XRD spectra of the starting slags. The starting eastern coal slag was amorphous, while the starting western coal slag was partially crystalline. Western coal slag segregated into two parts after being re-melted in a CO/CO<sub>2</sub> atmosphere: a crystalline part and a non-crystalline one. The major crystalline phases were determined to be Ca<sub>2</sub>Al<sub>2</sub>SiO<sub>7</sub> (gehlenite), Ca<sub>2</sub>MgSi<sub>2</sub>O<sub>7</sub> (akermanite), FeAl<sub>2</sub>O<sub>4</sub> (Hercynite) and MgAl<sub>2</sub>O<sub>4</sub> (spinel). In order to mix the two parts well for viscometry experiment, the western coal slag was crushed into fine powder and ball milled for 2 days.

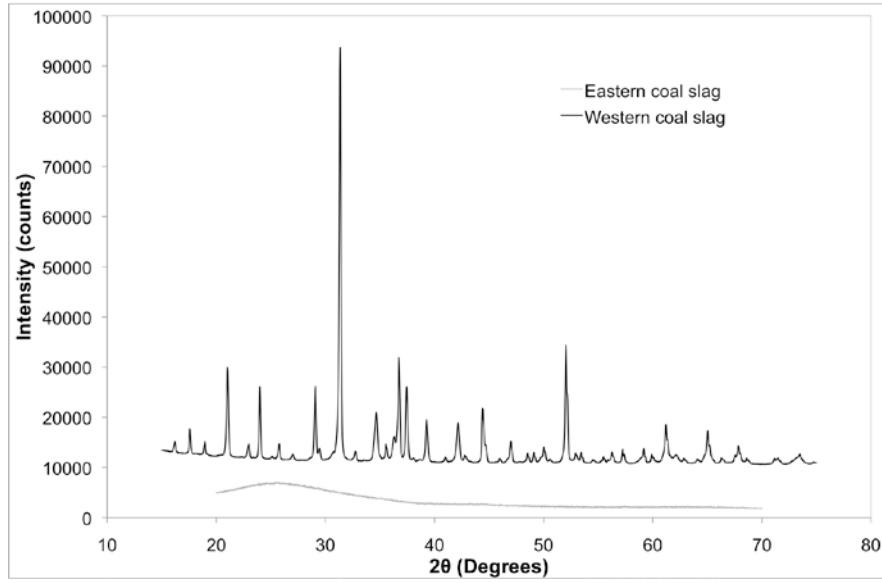


Fig. 1 XRD of the starting slags of eastern and western coal slag.

A combination of spindle and crucible materials was used and is listed in Table 2. The iron spindles and crucibles were machined from 1018 steel (0.18% C). The gas atmospheres were either a pre-prepared mixture of CO/CO<sub>2</sub> with a ratio of 1.8 or Ar (ultra high purity) purified through a getter system of heated Mg turnings. All the gases were supplied by Valley National Gas, Inc.

Table 2 Materials and atmospheres used in this study

Measurement No.	Slag	Spindle	Crucible	Atmosphere
EC-B1-M0	fresh	iron	ZrO <sub>2</sub>	Ar-5%H <sub>2</sub>
EC-B1-M1	fresh	iron	ZrO <sub>2</sub>	Ar (purified)
EC-B1-M2	recycled from measurement 1	iron	iron	Ar (purified)
EC-B1-M3	recycled from measurement 2	iron	iron (used in measurement No.2)	Ar (purified)
EC-B2-M1	fresh	Al <sub>2</sub> O <sub>3</sub>	Al <sub>2</sub> O <sub>3</sub>	CO/CO <sub>2</sub>
EC-B2-M2	fresh	Al <sub>2</sub> O <sub>3</sub>	ZrO <sub>2</sub>	CO/CO <sub>2</sub>
EC-B2-M3	fresh	Al <sub>2</sub> O <sub>3</sub>	Al <sub>2</sub> O <sub>3</sub>	UHP Ar (purified)
WC-B1-M1	fresh	Al <sub>2</sub> O <sub>3</sub>	Al <sub>2</sub> O <sub>3</sub>	CO/CO <sub>2</sub>
WC-B1-M2	fresh	Al <sub>2</sub> O <sub>3</sub>	ZrO <sub>2</sub>	CO/CO <sub>2</sub>

## 2.2 Measurement

### • Viscosity Measurement

The experimental setup is shown in Fig. 2. The viscosity measurements were carried out using the rotating cylinder method. The core component of the viscometer is the Brookfield Rheometer (model DV-III). The rheometer has a control unit that controls the rotation speed of the spindle, measures the torque exerted on the spindle and convert the information into a viscosity reading. The full-scale torque of the viscometer is  $7.187 \times 10^{-4}$  N·m. The rheometer can also be moved up and down along a guide rail, and the magnitude of such movement measured using a micrometer. The entire rheometer assembly is bolted onto a supporting platform inside an enclosure that is airtight.

The crucible filled with slag was steadily held by a set of three alumina rods and enclosed in an alumina protection tube attached to a metal flange. A thermocouple was placed in contact with the wall of the crucible, whose reading was used by a Eurotherm (Model 818) temperature controller to control the output power to the heating elements. The CO/CO<sub>2</sub> gas flows into the alumina protection tube through a gas introduction tube located next to the crucible, then escapes from the gas outlet built into the support platform. Iron and Al<sub>2</sub>O<sub>3</sub> spindles of the same dimensions were used in the measurements.

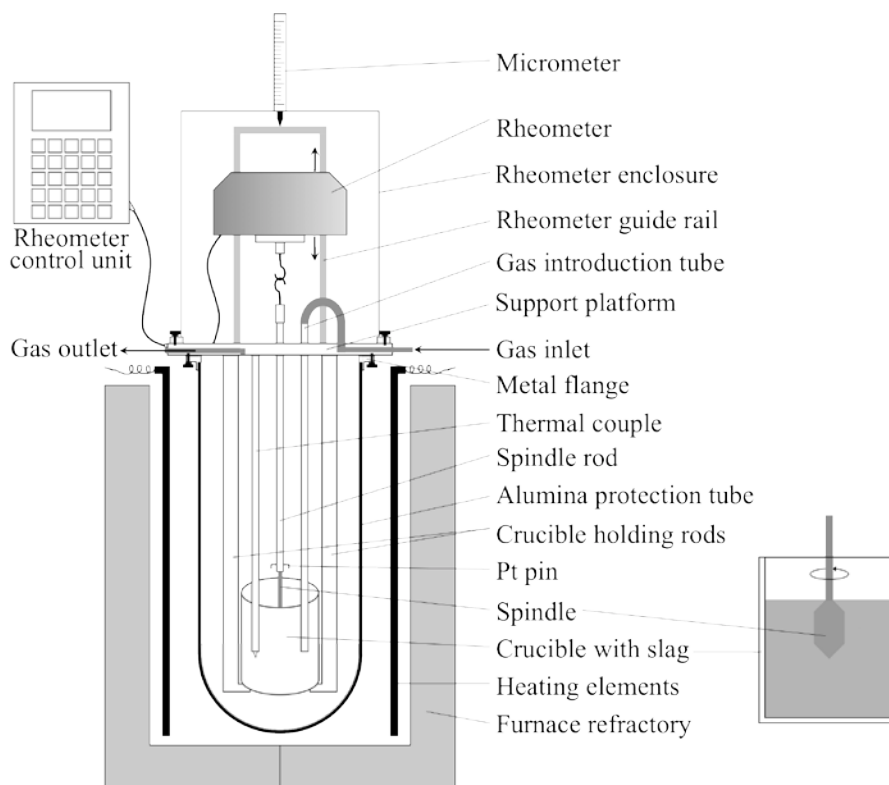


Fig. 2 Schematic of viscometer setup.

The viscometer was calibrated at  $298 \pm 0.1\text{K}$  before each measurement using three oil standards with viscosities of 4.95 Pa·s, 12.16 Pa·s and 58.56 Pa·s.

In a general measurement, after placing the crucible with the pre-melted slag onto the beaker holding rods and mounting the spindle onto the spindle rod, the alumina protection tube was sealed by bolting the metal flange to the supporting platform. The spindle was suspended about 3 cm above the crucible top by raising or lowering the rheometer along the guide rail by motorized drive. Before heating, the reaction chamber was flushed with CO/CO<sub>2</sub> gas for one hour. A continuous flow of the reaction gas was maintained to a flow rate of  $0.2 \pm 0.01$  l/min during the entire course of the measurement.

The slag was heated to the designated temperature using the temperature profile pre-programmed into the temperature controller. The initial heating rate was 5 K/min. Once the targeted temperature was reached, the slag was isothermally held to allow for stabilization. Next, the rotating spindle (typically at 5 rpm) was lowered toward the top of the liquid slag slowly until a sudden increase in the torque was read, which indicated the top of the melt was reached by

the tip of the spindle. The spindle was then lowered 16 mm, and the slag/spindle system maintained at the same temperature for 30 min to allow the system to thermally stabilize.

When thermal equilibrium was obtained, viscosity measurements were carried out in a step-cooling cycle of 25 °C increments. For each temperature, the rotation rates were adjusted to achieve a roughly constant torque value between 70-80%. Once the torque reading oscillated less than  $\pm 0.3\%$ , the viscosity value was obtained by averaging within the oscillating range.

After the viscosity was measured at the lowest temperature, typically 1300°C, the spindle was lifted to the starting position and the slag was rapidly cooled to room temperature. The slag composition was analyzed by XRF and XRD before and after each measurement. The slag/crucible and slag/spindle interfaced were also characterized with SEM.

### • Crystallization of Western Coal Slag

As noted in Fig. 1, the western coal slag showed a tendency to crystallize, while the eastern coal slag did not. In order to assess the crystallization tendency of the western coal slag, a confocal scanning laser microscope (CSLM) was used for the study of the crystallization that had a gold image hot stage attached to the microscope. This system had fast heating and cooling capabilities. Details of the CSLM has been documented in literature, but the key features of the system are (i) confocal optics with a source of He-Ne laser (with a wavelength of 632.8 nm) allowing for imaging of features in a narrow focal plane while filtering background glare due to radiation and (ii) an infra red heating system which allows for rapid heating and cooling. Using this system, the in-situ visualization of crystal precipitation in semi-transparent slags or on the surface of opaque slags could be observed.<sup>[9,10,11,12]</sup>

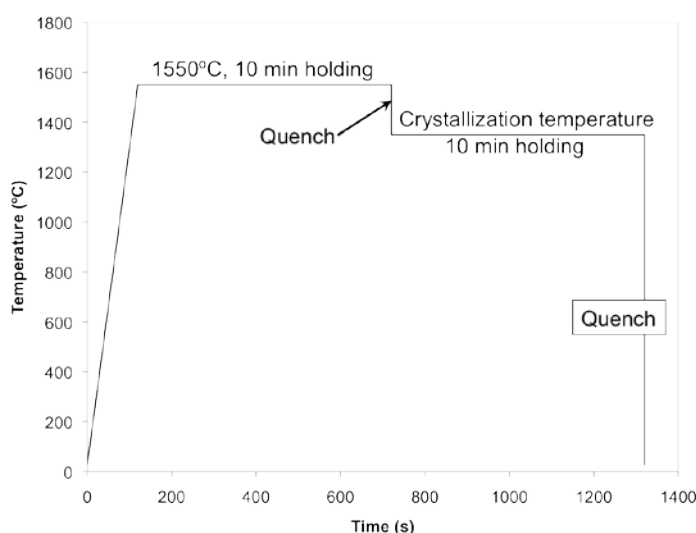


Fig. 3 Temperature profile used for the crystallization study.

typically in a few seconds, and held isothermally for another 10 minutes. The slag crystallization event was optically observed and recorded in situ and the time needed for the precipitation to occur on the surface of the slag liquid was recorded for each temperature. After crystallization occurred at each crystallization temperature, the slags were quenched to room temperature to evaluate the crystallized phases using the SEM and XRD.

### 3. Results

- **Eastern Coal Slag**

Fig. 4 shows the results of the viscometry experiments carried out for the eastern coal slag (EC), which is plotted along with model predictions according to references.<sup>[2,6,7]</sup> Since the composition of the slag did not change significantly after the viscosity measurements, it was reasonable to calculate the model viscosity values using starting slag composition listed in Table 1a.

The following trends can be noted:

- (i) The experiments carried out with all ceramic parts closely matched the predictions by FactSage, and to a lesser extent with the model by Kolmanovitch. At lower temperatures however, the Kolmanovitch model appears to approach the experimental data better.
- (ii) Measurements conducted using  $\text{Al}_2\text{O}_3$  and  $\text{ZrO}_2$  containers gauged similar/nearly identical viscosity values.
- (iii) In measurements carried out using an iron spindle and crucible in an inert atmospheres, viscosity values were consistently higher.
- (iv) The measurements obtained using an iron spindle and a ceramic container fall between the all ceramic and all iron systems.
- (v) When ceramic parts were used for viscosity measurements, the atmosphere was not found to have a noticeable affect on the viscosity.

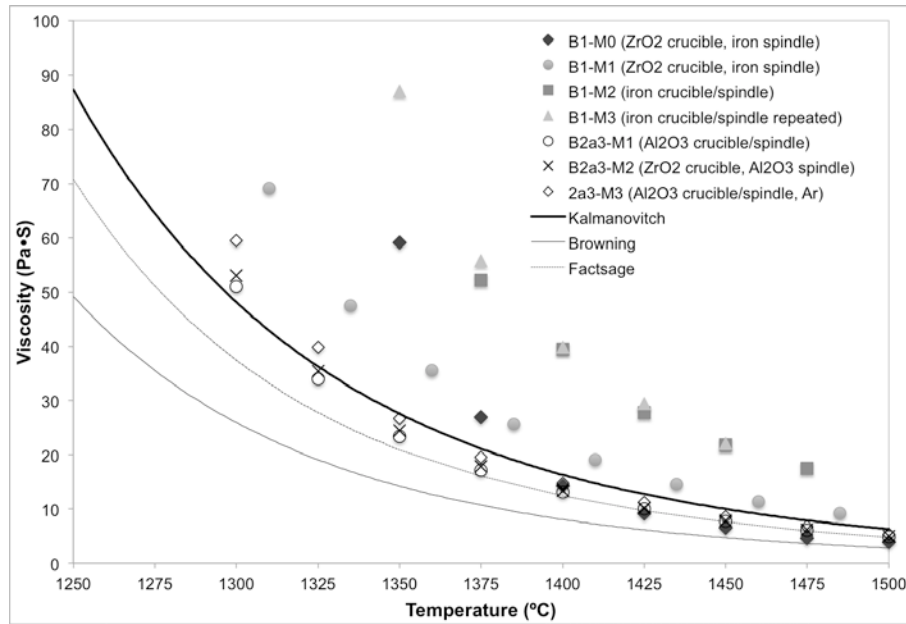


Fig. 4 Measured and predicted viscosity vs. temperature for the eastern coal slag.

The chemical analysis results of the spent slags after the viscosity measurements are listed in table 1 and showed that the bulk slag compositions did not change appreciably. When ceramic crucibles/spindles were used, the post-measurement slags picked up small amounts of  $\text{Al}_2\text{O}_3$  or  $\text{ZrO}_2$ , which was the inevitable result of dissolution of crucible/spindle material into the slag during viscosity measurement. No large change in the Fe content in the spent slag was noted. However, the chemical analysis could not indicate whether there was metallic Fe or ionic Fe in the slag. It was thought that the change in the bulk slag chemistry appeared to be small regardless of the system. It should be noted,

however, that the slags were nearly saturated in  $\text{Al}_2\text{O}_3$ , which would account for the small  $\text{Al}_2\text{O}_3$  container dissolution.<sup>[13]</sup>

Fig. 5 shows the post experiment characterization of slag/iron-crucible interfaces. The slag/iron-spindle interface had a very similar morphology. Fig. 5a shows significant amounts of metallic Fe at the crucible interface and entrained within the slag. The oxygen partial pressure in purified UHP Ar was determined by a  $\text{ZrO}_2$  oxygen sensor to be on the order of  $10^{-18}$  atm. The additions of Fe in the system could be a result of Fe precipitation from the slag since the oxygen potential was low enough to thermodynamically favor such a reaction. Kinetically, the decomposition of Fe-oxide to Fe, in the absence of a reducing agent (such as carbon), would be expected to be very slow or even negligible. For that reason it was surprising to find a minor amount of metallic Fe forming at the slag/crucible interface. Alternatively, metal could be entrained into the slag from the container walls, which was thought unlikely to have occurred since a metallic surface would not spall, especially below the fusion temperature of Fe.

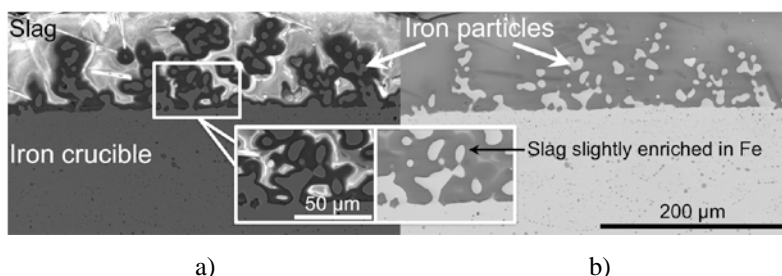


Fig. 5 a) Secondary electron (SE) and b) backscattered electron (BSE) images of the slag/iron-crucible wall.

In the case of the ceramic containers, the slag interacted with both  $\text{Al}_2\text{O}_3$  and  $\text{ZrO}_2$  crucible walls, but in different manners. Fig. 6a shows needle-shaped crystals precipitate along the  $\text{Al}_2\text{O}_3$  crucible wall. The EDS analysis indicated these crystals were most likely mullite ( $\text{Al}_6\text{Si}_2\text{O}_{13}$ ). XRD analysis on the post-measurement slag also showed the presence of both  $\text{Al}_2\text{O}_3$  and spinel phases. Therefore, the crystal formation could be a cooling effect.<sup>[14]</sup> On the other hand, the slag penetrated into the crucible wall, as can be seen in Fig. 6b. The depth of such penetration averaged around 1~2 mm. EDS analysis revealed that there was no significant change in  $\text{Al}_2\text{O}_3$  and FeO contents of the slag near the crucible wall.

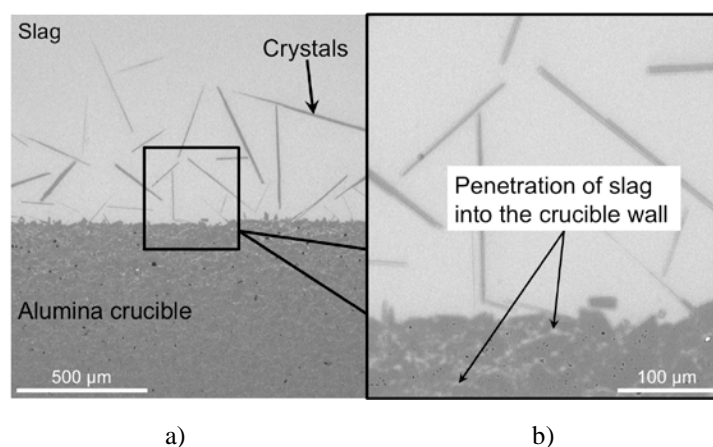


Fig. 6 a) SEM micrograph of a) slag/ $\text{Al}_2\text{O}_3$  crucible interface and b) penetration of slag into the crucible wall.



Fig. 7a shows the slag/ZrO<sub>2</sub>-crucible interface. Fig. 7b indicates that there is an increase in slag dissolving in the ZrO<sub>2</sub> crucible on the sidewalls, but it is not dramatic, and indeed the ICP results in Table 1 did not show any appreciable change in the bulk slag composition.

Thus, as far as the slag/solid reactions on the crucible, both the Fe and ceramic systems resulted in un-wanted phases, but when examining the data sets in Fig. 4, the use of the Fe-based materials caused a larger deviation from the predicted results. The inert atmosphere is required for using Fe viscosity components, but as seen in Fig. 5a, the reduction of FeO from the slag is significant. In the slags investigated, the oxidation state of Fe-ions is the same in Ar or in the CO/CO<sub>2</sub> ratio found in gasifiers (ratio of 1.8). A CO/CO<sub>2</sub> gas environment needs to be used when extending the study to slag mixtures that include V-oxides found in petcoke to ensure the desired oxidation state in Fe and V is achieved. Iron would not be stable when the CO/CO<sub>2</sub> ratio is 1.8. Therefore, based upon these interactions, it was decided that the ceramic systems would be the most suitable for the conditions of this study. Based on this, data sets EC-B2-M1, EC-B2-M2 and EC-B2-M3 were believed to be correct and agreed well with FactSage prediction until the temperature was below 1375 °C.

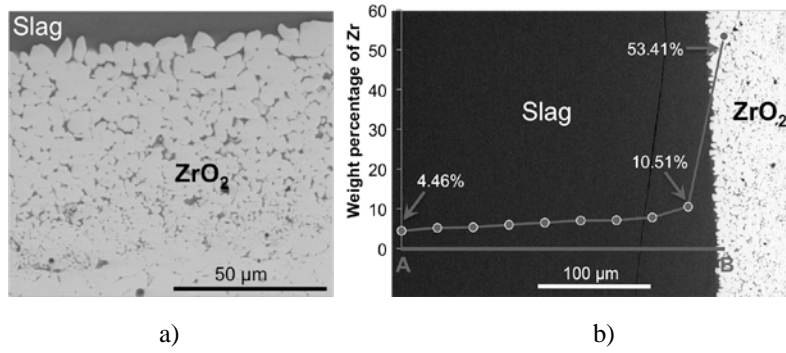


Fig. 7 a) backscattered electron image of slag/ZrO<sub>2</sub>-crucible interface; b) Zr composition profile along line AB

Fig. 8 below shows the natural log of viscosities vs 1/T plot for eastern coal slags. The activation energies listed in this graph are based upon the following equation:

$$\eta = A \exp\left(\frac{Q}{RT}\right) \quad (1)$$

where  $\eta$  is viscosity in Pa·s,  $Q$  is activation energy in joules and  $R$  is the gas constant. The viscosity datasets measured with all ceramic materials showed similar activation energies while those measured with iron spindle/crucible were higher. However, due to the formation of metallic Fe on the crucible/spindle, it is not appropriate to regard activation energies from such measurements as the activation energy of viscosity.

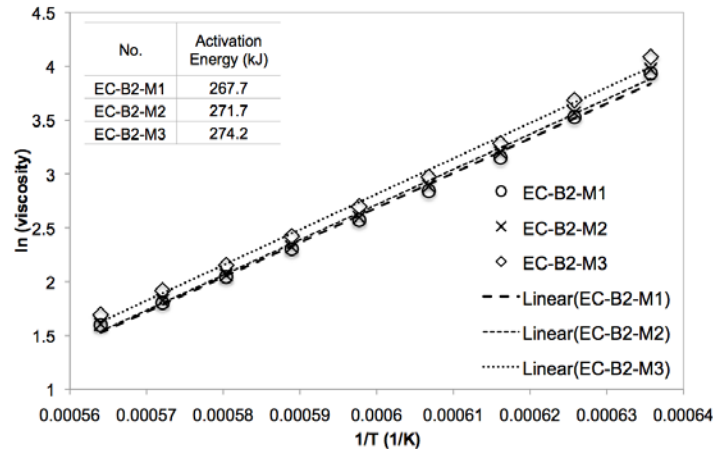


Fig. 8 Natural log plot of viscosities for eastern coal slags

### • Western Coal Slag

Western coal describes feedstock originating from the west of the Mississippi river. The western coal slag typically contains higher CaO and MgO contents than the slags from feedstock found further East. The increased concentrations of the alkali earth metal oxides cause the slag to have substantially different fusion temperatures, fluid properties, and chemical affinities toward refractory materials than its eastern coal slag counterpart. For this reason, the viscosity of western coal slag requires comparison to that of the eastern coal slag.

Fig. 9 plots the results of the viscosity measurements for the western coal slag (WC). The predicted viscosity values were calculated using the same models as in the eastern coal slag study. However, because of the aggressive nature of the western coal slag, the slag composition had changed significantly after each viscosity measurement due to dissolution of the crucible/spindle material, as seen in Table 1. Hence, the model viscosity values were calculated using slag compositions of both before and after the measurements. The  $ZrO_2$  content in the post-measurement slag was ignored for the following reasons: (i) none of the models considered in this paper took  $ZrO_2$  into account; (ii)  $ZrO_2$  has been reported to have little effect on the viscosity.<sup>[15]</sup>

It is noted in Figure 9 that the two measurements agreed best with the viscosity predictions of Kolmanovitch's model when calculated using a starting slag composition. For measurement one (WC-B1-M1), the viscosity dataset was characterized by an inflection point around 1350°C, which was more evident in the natural plot shown in Fig. 10. It was observed during the measurement that for temperatures above 1375°C, the molten slag was Newtonian, i.e. the relationship between the torque and rotation speed of the measuring head was linear; whereas the slag was non-Newtonian below 1350°C. The viscosity measured with  $ZrO_2$  crucible, WC-B1-M2, showed very different characteristics. Instead of a single inflection point, there was a bump in the temperature range of 1400~1350°C, which corresponded to the plateau in the natural log plot in Fig. 10. Upon examination of the post-experiment slags, it was believed that the different slag behavior in the two measurements was largely caused by the different crystallization behavior of the slags contained in the different crucibles, i.e.  $Al_2O_3$  and  $ZrO_2$  crucible materials.

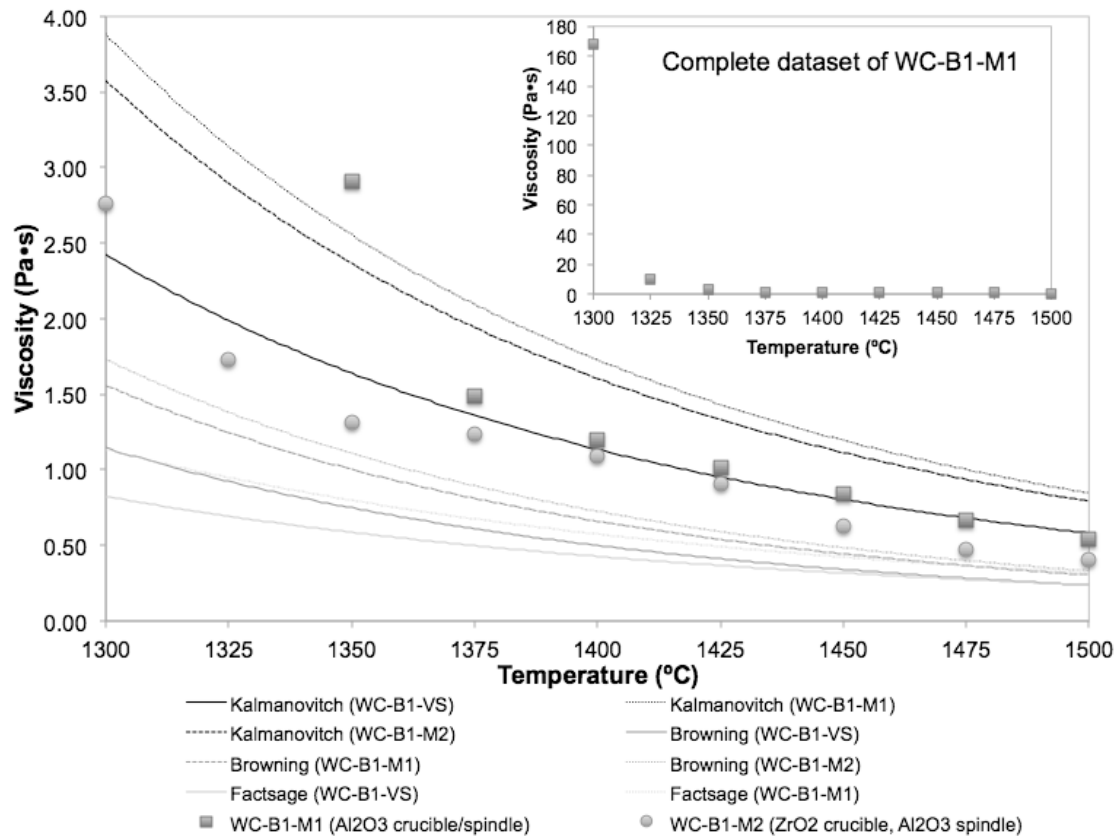


Fig. 9 Measured and predicted viscosity vs. temperature for the western coal slag (WC)

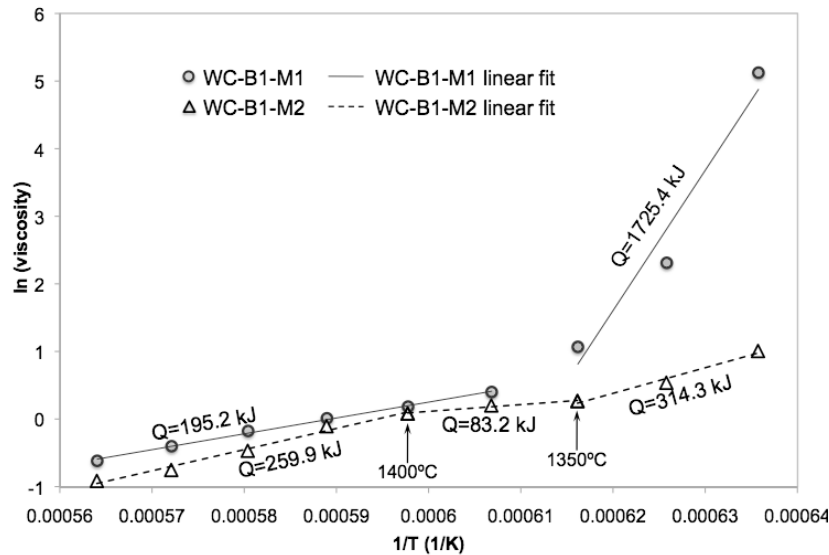


Fig. 10 Natural log plot for the two western coal slag viscosity measurements.

Fig. 11 shows the crucibles after the two viscosity measurements. An  $\text{Al}_2\text{O}_3$  crucible was used in measurement 1 (WC-B1-M1), and a  $\text{ZrO}_2$  crucible in measurement 2 (WC-B1-M2). Firstly, it was evident in Fig. 11a and b that both crucibles were attacked by the slag, which resulted in significant dissolution of the crucible materials. Secondly, although the slags were quenched in the same manner in the two measurements, the crystallization of the slags was very different, because the materials introduced into the slag played different role in terms of crystallization.

The slag in the  $\text{Al}_2\text{O}_3$  crucible was almost completely crystalline, see Fig. 11a. At the crucible/slag interface, dissolution resulted in an  $\text{Al}_2\text{O}_3$  saturated slag layer was indicated by SEM-EDS evaluation at the region labeled S in Fig. 11c. XRD identified the major crystalline phases in the bulk slag to be  $\text{Ca}_2\text{Al}_2\text{SiO}_7$  (gehlenite),  $\text{Ca}_2\text{MgSi}_2\text{O}_7$  (akermanite),  $\text{FeAl}_2\text{O}_4$  (hercynite) and  $\text{MgAl}_2\text{O}_4$  (spinel). Moreover, comparing the XRD patterns of the slag before and after the first measurement, the relative intensity and positions of some peaks changed slightly. The peak shifts were associated with aluminum containing phases, i.e. gehlenite, hercynite and spinel. The introduction of  $\text{Al}_2\text{O}_3$  from the crucible into the slag resulted in a significant change in the slag viscosity, and impacted the crystallization of the slag. The  $\text{Al}_2\text{O}_3$  crucible wall may also act as a nucleation site that assists crystallization. With significant amount of crystals precipitated, the slag viscosity changed from Newtonian to non-Newtonian.

The slag in the  $\text{ZrO}_2$  crucible (WC-B1-M2) was partly glassy with some visible crystals. As shown in Fig. 11d, unlike the slag in  $\text{Al}_2\text{O}_3$  crucible, the slag in  $\text{ZrO}_2$  crucible had only two crystalline phases:  $\text{ZrO}_2$  and  $\text{MgAl}_2\text{O}_4$ , as determined by SEM-EDS and XRD analyses. The two crystalline phases are indicated in Fig. 11d by “A” and “B”, respectively. Because of the dendritic morphology of the  $\text{ZrO}_2$  crystals, it was believed that  $\text{ZrO}_2$  dissolved into the slag at high temperatures and re-precipitated when measuring viscosity at lower temperatures or on cooling. Despite dissolution and re-precipitation,  $\text{ZrO}_2$  should have little impact on the viscosity of the liquid, particularly at higher temperatures.<sup>[15]</sup> The precipitation of  $\text{MgAl}_2\text{O}_4$  crystals fits thermodynamics prediction made with FactSage, as shown in Fig. 13. It was also noted that the  $\text{Al}_2\text{O}_3$  spindle in the second measurement was attacked much more severely than the one used in the first measurement. The diameter of the spindle shrank from 11.94 mm to 10.39 mm. On a rough estimation, this would result in an approximately 16.9% decrease in the surface area of the spindle measuring head that was in contact with the slag at the end of the measurement, which would affect the torque measured.

Fig. 12 shows the TTT diagram of the crystallization of western coal slag. Crystals precipitated very fast at all the temperatures examined. This result showed that when the viscosity was measured, the melt was in fact a mixture of liquid slag and crystals. Although the TTT curve seemed to have two “noses”, the crystalline phase found at the two nose-temperatures had no difference. The crystalline phases predicted by FactSage are given in Fig. 13, which also show that the weight fraction of crystals in the melt should increase at lower with lowering temperatures. In the temperature range of 1200~1500°C, the only crystalline phase predicted and observed while obtaining TTT diagram was  $\text{MgAl}_2\text{O}_4$  spinel. An SEM micrograph of the crystals is shown in Fig. 13. Spinel crystals precipitated at higher temperatures were usually larger, but in a smaller amount than those precipitated at lower temperatures.

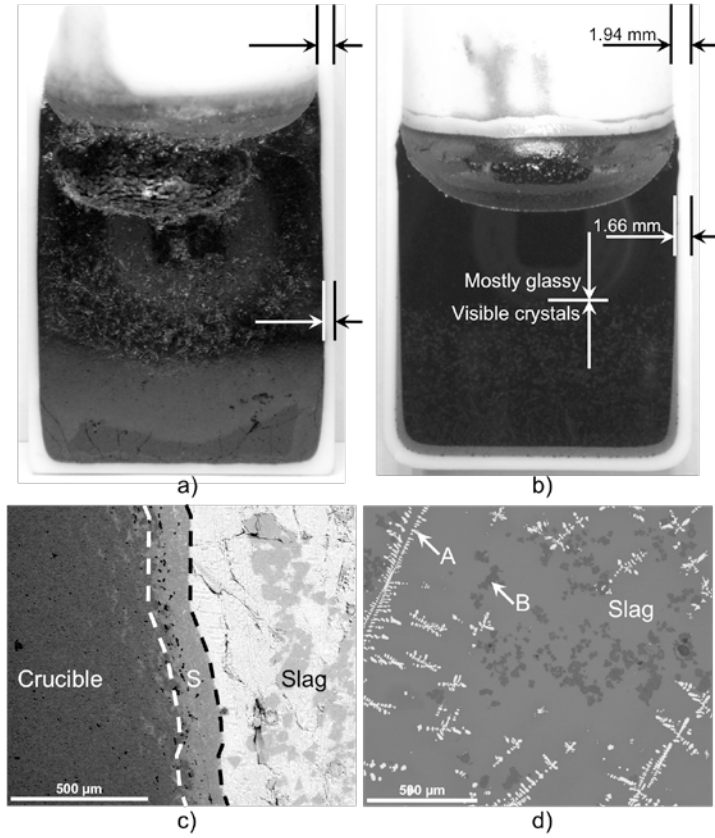


Fig. 11 Optical images of cross-sectioned and polished crucibles after viscosity measurement for a) WC-B1-M1 and b) WC-B1-M2; and backscattered electron SEM images of the post-measurement crucible and slag for c) WC-B1-M1 and d) WC-B1-M2.

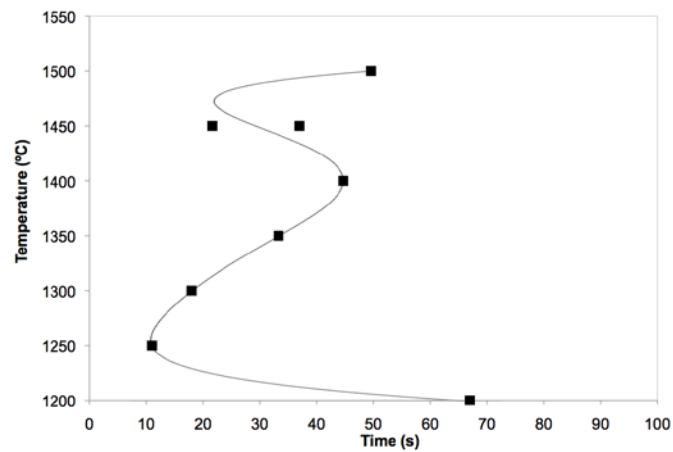


Fig. 12 TTT diagram for crystal precipitation in western coal slag under  $\text{CO}/\text{CO}_2 = 1.8$ .

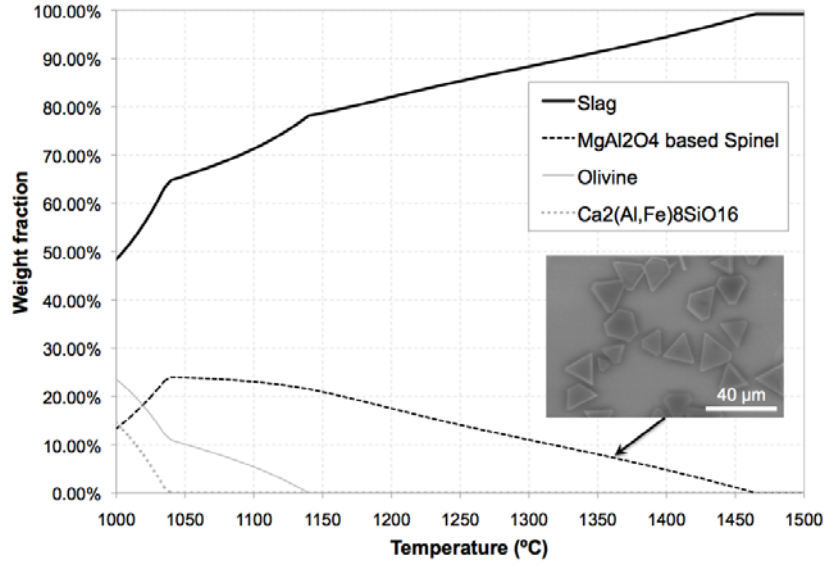


Fig. 13 The crystalline phases predicted by FactSage, and the SEM image of the crystals precipitated in WC.

The viscosity of a slag containing both liquid and solid,  $\eta_{\text{mixture}}$ , can be described by the Goldsmith equation:<sup>16</sup>

$$\eta_{\text{mixture}} = \eta_{\text{liquid}}(1 + ax + bx^2), \quad (2)$$

where  $x$  is the volume fractional of solid in the melt,  $\eta_{\text{liquid}}$  is the viscosity of the liquidus slag,  $a$  is a constant related to the shape of the crystal and/or crystal clusters, and constant  $b$  is related to solid-melt hydrodynamic interaction. Annen et al.<sup>[17]</sup> reported  $a = 2.5$  and  $b = 9.15$  for spherical solid at low concentrations.

As shown in Fig. 13, the only type of crystal present in the slag from 1500-1200°C was spinel, which had a shape that was either “equiaxed” polyhedron or truncated polyhedron, because of  $\{111\}$  faceting of spinel crystals.<sup>[18]</sup> Therefore, the shape of the crystals was approximated as a polyhedron, values for constants  $a$  and  $b$  could be obtained for the western coal slag with both experimental viscosity data and model prediction values. The viscosity in dataset WC-B1-M1 above 1350°C were chosen for  $\eta_{\text{mixture}}$ , because the viscosity vs temperature dependence of the WC-B1-M1 agreed fairly well with Kalmanovitch predictions calculated with the starting slag composition, and hence,  $\eta_{\text{liquid}}$  was taken as the Kalmanovitch prediction values. The weight percentage of phases calculated by FactSage, as shown in Fig. 13, was converted into volume fraction. The volume of the liquid slag was calculated using the method described by Mills et al.<sup>[19]</sup> Adopting the same form of equation (2), and fitting of the data for  $\eta_{\text{mixture}}$  and  $\eta_{\text{liquid}}$  results in the following equation with  $R^2 = 0.997$ :

$$\eta_{\text{mixture}} = \eta_{\text{liquid}}(1 + 2.8858x + 10.5618x^2) + (0.1543\eta_{\text{liquid}} - 0.1118), \quad (3)$$

Since the values of the last part of equation (3) are on the order of  $10^{-2}$ , equation (3) can be simplified into the following:

$$\eta_{\text{mixture}} = \eta_{\text{liquid}}(1 + 2.8858x + 10.5618x^2). \quad (4)$$

The values of constant  $a$  and  $b$  in equation (2) were 2.8858 and 10.5618, respectively, only slightly larger than those

reported by Annen.<sup>[17]</sup> One should also note that the Goldsmith equation can only serve as a first approximation to describe the effect of the precipitation of crystalline phase on the viscosity of slags because it does not take into account factors such as the size of crystallites.

In conclusion, viscometry experiment of western coal slag is challenging because such slag is corrosive to the ceramic container and spindle. Despite dissolution of container/spindle materials into the slag, the two viscosity datasets obtained agreed best with Kalmanovitch prediction values from 1375-1500°C. Precipitation of crystalline phase seems inevitable for this slag chemistry. Estimation of the constants in Goldsmith equation with experimental viscosity data resulted in reasonable values. Nevertheless, a more corrosion-resistant container/spindle material must be used to minimize the introduction of foreign substance into the slag; also its interaction with the slag should be minimal.

#### 4. Conclusions

Rotating bob-viscometer experiments were carried out on synthetic slags with chemistries similar to eastern and western coal slags. It was found that:

- (i) Iron containers and spindles used in inert atmospheres resulted in viscosity values larger than expected as a result of metallic Fe precipitation at the slag/solid walls, resulting in higher activation energy than expected.
- (ii) The use of ceramic materials ( $\text{Al}_2\text{O}_3$  or  $\text{ZrO}_2$ ) resulted in reasonable and reproducible viscosity data for eastern coal.
- (iii) The ceramic container and spindle were attacked by western coal slag and crystallization occurred during viscometry experiments for this slag chemistry. TTT study of crystallization showed that crystallization occurred fast in the temperature range of 1500-1200°C.
- (iv) An approximate relation between precipitation of crystalline phase and slag viscosity was obtained using Goldsmith equation.

#### Acknowledgement

This technical effort was performed in support of the National Energy Technology Laboratory's ongoing research in development of coal gasification under the RES contract DE-FE0004000.

**Disclaimer:** "This report was prepared as an account of work sponsored by an agency of the United States Government. Neither the United States Government nor any agency thereof, nor any of their employees, makes any warranty, express or implied, or assumes any legal liability or responsibility for the accuracy, completeness, or usefulness of any information, apparatus, product, or process disclosed, or represents that its use would not infringe privately owned rights. Reference herein to any specific commercial product, process, or service by trade name, trademark, manufacturer, or otherwise does not necessarily constitute or imply its endorsement, recommendation, or favoring by the United States Government or any agency thereof. The views and opinions of authors expressed herein do not necessarily state or reflect those of the United States Government or any agency thereof."

#### References

- [1] J.P. Bennett, K. Kwong, C. Powell, R. Krabbe, H. Thomas, and A. Petty. Low Chrome/Chrome Free Refractories

for Slagging Gasifiers. *Research Report DOE/NETL-IR-2006-119*, 2006, p 200-206.

- [2] G.J. Browning, G.W. Bryant, H.J. Hurst, J.A. Lucas, T.F. Wall. An Empirical Method for the Prediction of Coal Ash Slag Viscosity. *Energy & Fuels*, 2003, 17(3), p 731-737.
- [3] W.A. Selvig, F.H. Gibson. Analyses of Ash from United States Coals. *Bureau of Mines Bulletin 567*, United States Government Printing Office, Washington, 1956.
- [4] A. Kondratiev and E. Jak. Review of experimental data and modeling of the viscosities of fully liquid slags in the  $\text{Al}_2\text{O}_3$ -CaO-'FeO'- $\text{SiO}_2$  system. *Met. Trans. B*, 32B, 2001, p 1015-1025.
- [5] G. Urbain, F. Cambier, M. Deletter, M.R. Anseau. Viscosity of Silicate Melts. *Trans. J. Br. Ceram. Soc.* 1981, 80, p 139-141.
- [6] C.W. Bale, A.D. Pelton, and W.T. Thompson. *Facility for the Analysis of Chemical Thermodynamics*. Ecole Polytechnique, Montreal, <http://www.factsage.com>, 2000
- [7] D.P. Kalmanovitch, M. Frank. An Effective Model of Viscosity for Ash Deposition Phenomena. In Engineering Foundation Conference on Mineral Matter and Ash Deposition from Coal, United Engineering Trustees Inc., Santa Barbara, CA, 1988.
- [8] S. Vargas. Straw and Coal Ash Rheology. PhD Thesis, 2001, Technical University of Denmark.
- [9] J. Nakano, S. Sridhar, T. Moss, J. Bennett and K-S.-Kwong. Crystallization of Synthetic Coal&Petrocoke Slag Mixtures Simulating Those Encountered in Entrained Bed Slagging Gasifiers. *Energy & Fuels*, 23, 2009, p 4723-4733.
- [10] C. Orrling, S. Sridhar and A.W. Cramb. In situ observations and thermal analysis of crystallization phenomenon in mold slags. *High Temp. Mater. Processes*, 2001, 20(3-4), p 195-199.
- [11] C. Orrling, S. Sridhar and A.W. Cramb. In situ observation of the role of alumina particles on the crystallization behavior of slags. *ISIJ Int.*, 40, 2000, p 877-885.
- [12] S. Sridhar and A.W. Cramb. Kinetics of  $\text{Al}_2\text{O}_3$  dissolution in CaO-MgO- $\text{SiO}_2$ - $\text{Al}_2\text{O}_3$  slags: In situ observations and analysis. *Metall. Mater. Trans. B*, 2000, 31B(2), p 406-411.
- [13] H. Soll-Morris, C. Sawyer, Z.T. Zhang, G.N. Shannon, J. Nakano and S. Sridhar. The interaction of spherical  $\text{Al}_2\text{O}_3$  particles with molten  $\text{Al}_2\text{O}_3$ -CaO-FeO<sub>x</sub>- $\text{SiO}_2$  slags. *Fuel*, 2008, 88, p 670-682.
- [14] T.K. Kaneko, J.P. Bennett, and S. Sridhar. Effect of Temperature Gradient on Industrial Gasifier Coal Slag Infiltration into Alumina Refractory. *J. Am. Ceram. Soc.*, 2011, 94(12), p 1-9.
- [15] P. Hrma, B.M. Arrigoni, M.J. Schweiger. Viscosity of many-component glasses. *J. Non-Cryst. Solids*, 2009, 355, p 891-902.
- [16] H.L. Goldsmith, S.G. Mason. *Rheology, Theory and Application*. Academic Press, NY, 1967.
- [17] K. Annen, J. Gruninger, G. Stewart. Method for extending viscosity predicted formulas, *Proc. Flames Res. Found.* 1983, p 1-3.
- [18] C.B. Carter and Y.K. Rasmussen. Growth of Spinel Particles on Alumina Thin Films-i. Orientation Relationships and Shape of the Particles. *Acta Metall Mater.*, 1994, 42(8), p 2729-2740.
- [19] K.C. Mills and B.J. Keene. Physical properties of BOS slags. *Int. Mater. Rev.*, 1987, 32, p 1-120.